

Urbanization and Other Land Use Land Cover Change Assessment in the Greater Kumasi Area of Ghana

Addo Koranteng¹, Isaac Adu-Poku², Bernard Fosu Frimpong³, Jack Nti Asamoah⁴, John Agyei¹, Tomasz Zawila-Niedźwiecki⁵

¹Institute of Research, Innovation and Development, Kumasi Technical University, Kumasi, Ghana

²Geomatic Engineering Department, Kwame Nkrumah University of Science and Technology, Kumasi, Ghana

³Department of Hydrology, Brandenburg University of Technology, Cottbus, Germany

⁴Department of Civil Engineering, Faculty of Engineering and Technology, Kumasi Technical University, Kumasi, Ghana

⁵Coordination Centre for Environmental Projects, Warszawa, Poland

Email: addo.koranteng@kstu.edu.gh, i.adupoku@yahoo.com, bengarzy007@gmail.com, jack.nasamoah@kstu.edu.gh, tzawilan@gmail.com

How to cite this paper: Koranteng, A., Adu-Poku, I., Frimpong, B. F., Asamoah, J. N., Agyei, J., & Zawila-Niedźwiecki, T. (2023). Urbanization and Other Land Use Land Cover Change Assessment in the Greater Kumasi Area of Ghana. *Journal of Geoscience and Environment Protection*, 11, 363-383.

<https://doi.org/10.4236/gep.2023.115022>

Received: March 30, 2023

Accepted: May 28, 2023

Published: May 31, 2023

Copyright © 2023 by author(s) and Scientific Research Publishing Inc. This work is licensed under the Creative Commons Attribution International License (CC BY 4.0).

<http://creativecommons.org/licenses/by/4.0/>



Open Access

Abstract

Urbanization posits the expression of urban expanse expansion due to population growth, rise in built-up areas, high population density and its correspondingly urban way of life. Unrestrained impetus of development and land use land cover change (LULCC) portent several issues such as unlawful urban sprawl, loss of agricultural land, forest loss and other associated complications. This study analyzed the dynamics of urbanization and other LULCC in Ghana's Greater Kumasi area via Landsat images (TM 1986, OLI 2013 and OLI 2023) using ERDAS Imagine, Idrisi and ArcGIS software. Implementing supervised classification technique, the Maximum Likelihood Classifier (MLC) procedure was employed to categories the study area into five LULC classes. Accuracy assessment undertaken on the resultant LULC maps was deemed very satisfactory. The results from 1986-2023 pointed to an upsurge in a built-up extent as of 8% to 41%, a decrease in Closed Forest from 9% to 4%, another decrease in Open Forests from 64% to 33%, a slight increase from 16% to 20% in farmlands and a stable level of water share. Further analysis indicated that the study area had undergone LULCC within the periods 1986-2013 and 2013-2023 at 60% and 37% respectively. The findings showed uncontrolled urban sprawling along major roads and forest loss as deforestation outside protected areas and degradation in protected forest. The monitoring of urbanization and other LULCC is important for local, and national governments and other bodies charged with the implementation of programs

and policies that manage and utilize natural resources. Development adapts to mitigate the effect on the environment.

Keywords

Urbanization, Maximum Likelihood Classifier (MLC), Urban Sprawl, Change Detection, Forest Loss

1. Introduction

Urbanization remains one of the most active and vital subjects in contemporary times since rapid expansion has mostly ensued in the disorganized and unintended development of cities with its dire consequences of other LULCC and ecosystem services role played by the flora and fauna in any given area (Ioja & Qureshi, 2020; Pal et al., 2023). A number of studies have demonstrated that urbanization is a development whereby valuable farmland, forest and surface water categories are being permanently decreasing and outrightly being lost (Muhammed & Emigilati, 2019; Weslati et al., 2023).

Deforestation and Climate change remain global issues which are impacted greatly by LULCC. LULCC has consequently been identified as a crucial part of ecological transformation on all spatiotemporal scales (Bufebo & Elias, 2021; Naboureh et al., 2021). Thus, LULCC monitoring is pivotal for community, provincial, national and even international level designing and implementing strategies in order to assess urban growth trends (Grigorescu et al., 2021; Wiatkowska et al., 2021). Precise in addition to up-to-date information are necessities for the detection, monitoring, and analysis of the variations in the urban LULC patterns for efficient and effective management (Sun et al., 2007; Hersperger et al., 2018). Largely, anthropogenic activities are reckoned to be liable for compelling the modifications resulting in altered environments which adversely influence terrain and its attendant resources (Benson, 2019; Makwinja et al., 2021).

To be able to quantify changes in any environment, change detection is an important exercise that must be undertaken. Change detection is explained as the means of pinpointing changes in the condition of an environmental element by examining it at various times (Shi et al., 2020; Khelifi & Mignotte, 2020; Peng et al., 2020). Satellite imagery provides excellent means to study change detection. Landsat images especially, and other satellite images such as Disaster Management Constellation (DMC) and Sentinel have been employed by several researchers in the study of LULCC in the study area (Asori & Adu, 2023; Koranteng et al., 2021; Frimpong et al., 2023; Asabere et al., 2020; Koranteng et al., 2020).

Numerous research papers have established the pertinence of remote sensing (RS) and geographic information systems (GIS) in urbanization and LULCC studies (Atay Kaya & Kut Görgün, 2020; Sibanda & Tsuyuki, 2022; Olorunfemi et al., 2020). The primary aim of this paper is to assess urbanization and other LULCC over 37 years (1986-2023) period and its connection with population in

Greater Kumasi Area in Ghana. This paper uses several existing methodologies to address teething challenges in the study area.

2. Methodology

2.1. Study Area

The study area (**Figure 1**) is located centrally within the Ashanti Region which includes Kumasi (capital) and its immediate bordering districts (Atwima Kwanwoma, Afigya Kwabre, Kwabre, Atwima Nwabiagya, Bosomtwe and Ejisu Juaben). The study area falls within the coordinates—longitude $1^{\circ}58'W$ & $1^{\circ}11'W$ and latitude $6^{\circ}22'N$ & $7^{\circ}11'N$. Ashanti Region has the highest population in Ghana over the past decades until recent 2021 population census where its second to Greater Accra (GSS, 2022). The 2021 population of the region stood at 5,440,463 at a 3.8% growth rate (**Table 1**).

The study area is located within the middle belt of Ghana and lies within the tropical rainforest zone. The study area is endowed with Owabi Wildlife sanctuary, Lake Bosometwi and Bobiri Forest Reserve. Ashanti region experiences both wet and dry climate conditions throughout the year. The rainfall pattern in the area commences in March and end in November, which peaks in May-June and October. The average annual rainfall is 1400 mm at an average annual temperature of $29^{\circ}C$.

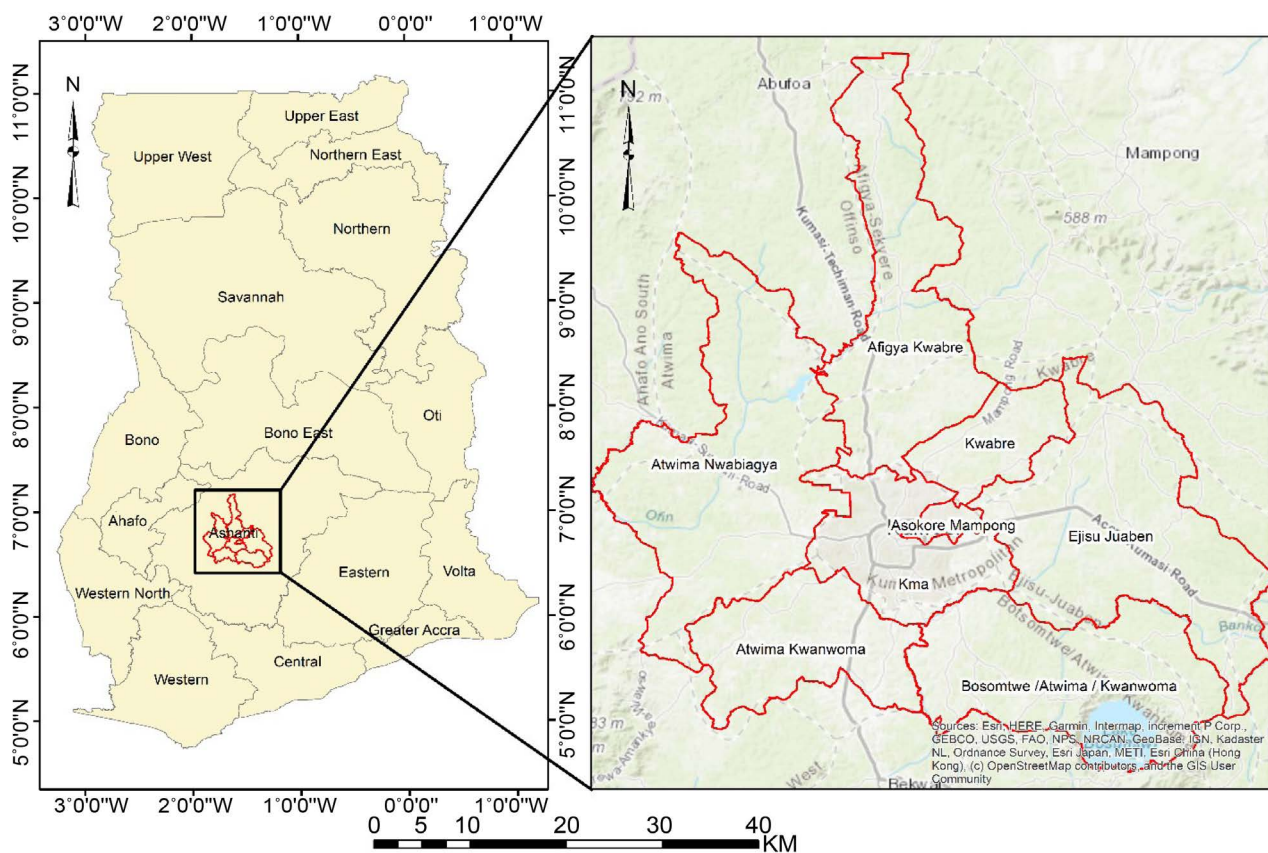


Figure 1. Study area comprising the old Kumasi metropolitan assembly, and adjoining districts.

Table 1. Ghana's population and Ashanti region shares, 1960-2021 (GSS, 2022).

Year	Total (Ghana)		Ashanti	
	Size	%	Size	%
1960	6,726,815	100.00	1,109,133	16.3
1970	8,559,313	100.00	1,481,698	17.3
1984	12,296,081	100.00	2,090,100	17.0
2000	18,912,079	100.00	3,612,950	19.1
2010	24,658,823	100.00	4,780,380	19.4
2021	30,832,019	100.00	5,440,463	17.6

Source: Ghana statistical service.

The study area is gifted with some hilly areas with a mean elevation of 250 m above Mean Sea Level (MSL). The main water source within the study area are the natural lake, dams and several rivers. Kumasi populace draw their potable water from the Owabi and Barekese head works.

2.2. Material & Data

Table 2 lists the data sources used in this research and grouped into two: Earth observation (EO) data and reference data. For this study, Landsat satellite images were used to analyze LULCC as it provides multi-temporary capability. Landsat images were downloaded from the USGS Earth Explorer website (<http://glovis.usgs.gov/>) which covers Path/Row scenes 194/55 and 194/56 of the study area. These images were selected based on date acquisition, availability and less than 10% cloud cover. The other data that forms the reference data contain aerial photographs, topographical maps, Landuse maps and 2012 ground truth data of the study area.

2.3. Methods

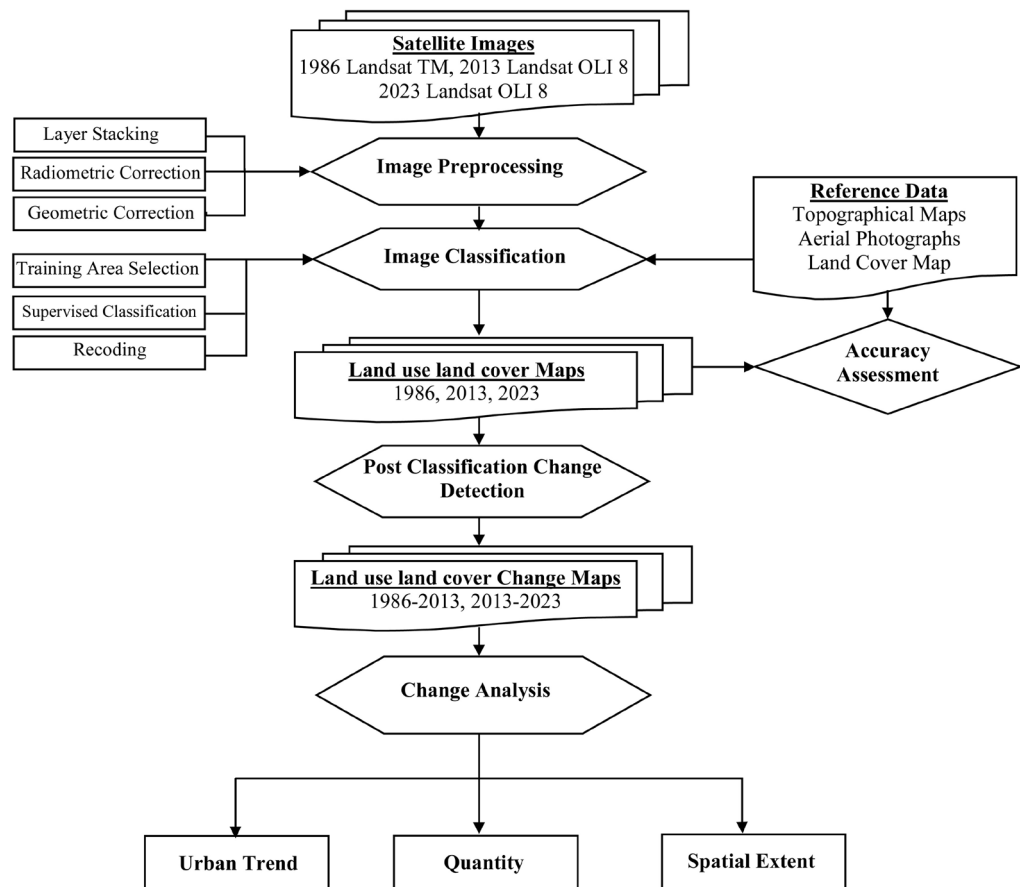
Figure 2 summarized the methods adopted in this paper as illustrated in the flow chart and have been elaborated in the subsequent sub-sections.

2.3.1. Image Pre-Processing

Image pre-processing serves as essential process in removing systematic and unsystematic errors that are attributed to certain effects arising from sensors, atmosphere and the Earth's curvature. Image pre-processing is the first process done to reduce system errors and atmospheric effects in sensors uncorrected errors, if not rectified leads to false results in change detection analyses (Kamuso-ko, 2019; Phiri et al., 2018). Layer stacking was performed on the downloaded Landsat images (1986, 2013 and 2023) and clipped accordingly to Area of Interest (Study Area). The resultant 1986 Landsat image was found to be hazy and was therefore corrected. All the resultant images were subsequently enhanced using Histogram Equalization.

Table 2. Satellite data used for LULC classification and reference data.

EO Data	Acquisition date	Resolution	Source
Landsat TM	December, 1986	30 m	USGS EROS Centre
Landsat OLI 8	March, 2013	30 m	USGS EROS Centre
Landsat OLI 8	January, 2023	30 m	USGS EROS Centre
Reference Data			
Topographical Map	2012	1:50,000	Survey & Mapping Division, Ghana
Aerial Photographs	2010	1:10,000	Survey & Mapping Division, Ghana
Land Cover Map	1986	30 m	CERGIS, University of Ghana
Land Cover Map	2010	30 m	RMSC - Forestry Commission, Ghana
Training Data (FPP)	2012		RMSC - Forestry Commission, Ghana

**Figure 2.** Methodology flowchart adopted in the study.

2.3.2. Image Classification

To extract the various LULC classes, training and validating data are needed to obtain accurate classification of the study area. Desktop review was first carried out which includes obtaining all the relevant data and information of the study area. In all, 250 ground truth data evenly distributed were collected at random from the study area. Based on the number of LULC classes identified, 50 training points out of the total together with other reference data (local knowledge, aerial photo and Google Earth images) of the study area, the 2023 Landsat image were categorized. Accuracy assessments of the classified image were hence performed with the other 200 ground truth points. The 2013 satellite image was classified based on the ground truth data acquired from the Forestry Commission, Ghana and the 1990 landcover map of Ghana acquired from CERGIS was used to classify the 1986 satellite image.

Based maximum likelihood algorithm supervised classification, the study area was grouped into five (5) LULC categories: 1) Built-up; 2) Close Forest; 3) Open Forest; 4) Farmland and 5) Water as indicated in **Table 3**. The maximum likelihood algorithm adopted in this study was based on a function proposed by (Richards, 1999):

$$g_i(x) = \ln p(\omega_i) - \frac{1}{2} \ln |\Sigma_i| - \frac{1}{2} (x - m_i)^T \Sigma_i^{-1} (x - m_i) \quad (1)$$

where:

i = class;

x = n-dimensional data (where n is the number of bands);

$p(\omega_i)$ = probability that class ω_i occurs in the image and is assumed the same for all classes;

$|\Sigma_i|$ = determinant of the covariance matrix of the data in class ω_i ;

Σ_i^{-1} = its inverse matrix;

m_i = mean vector.

2.3.3. Accuracy Assessment

Accuracy assessment shows how classified images correctly compare with reference or ground truth data. Accuracy assessment evaluates the quality of the

Table 3. Classification scheme of LULC used in this study.

Land use Class	Feature
Closed Forest	Land with dense woody tree cover with close canopy and forest patches.
Open Forest	Land with dense woody tree cover without close canopy. Forest Land in the national greenhouse gas inventory that are degraded.
Farmland	Cultivated land and harvested croplands and pastures
Built Up	Land with non-natural surface such as roads and highways, built up areas, bare grounds and human settlements
Water	Rivers, Streams, reservoirs, ponds, and lakes

thematic map and should not be less than 80% (Congalton, 1991, Anderson et al., 1976). This study employed confusion matrix algorithm and Kappa statistics to perform the accuracy assessment on the classified images. The 1986 LULC accuracy assessment could not be performed as there were no available reference data. Morshed et al., 2022 proposed the below-mentioned equations used in computing accuracy assessment parameters and Table 4 summarized the confusion matrix and the kappa statistics calculated.

$$\begin{aligned} & \text{Producer accuracy (\%)} \\ &= \frac{\text{No. of correctly classified pixels (diagonal)}}{\text{Total no. of reference pixels in each category (column)}} \times 100 \end{aligned} \quad (2)$$

$$\begin{aligned} & \text{User accuracy (\%)} \\ &= \frac{\text{No. of correctly classified pixels in each category}}{\text{Total no. of reference pixels in each category (row)}} \times 100 \end{aligned} \quad (3)$$

$$\begin{aligned} & \text{Overall accuracy (\%)} \\ &= \frac{\text{Total no. of corrected classified pixels (diagonal)}}{\text{Total no. of reference pixels}} \times 100 \end{aligned} \quad (4)$$

Kappa

$$= \frac{\text{Total sample number} \times \text{Total corrected sample number} \sum (\text{col. total} \times \text{row total})}{\text{Total sample number}^2 - \sum (\text{col. total} \times \text{row total})} \quad (5)$$

2.4. LULCC Analysis

Post-Classification Change Detection was adopted LULCC that have occurred within the 37 year period (1986-2023). The LCM module of Idrisi Selva, accept two LULC maps with the same dimensions at a time to perform cross-tabulation to analysis LULC changes. Using the 1986, 2013 and 2023 thematic maps as inputs in LCM module, the following were generated for the 1986-2013 and 2013-2023 time period: 1) LULC Net gains (+) or losses (-) in hectares (ha) and percentages (%); 2) change Maps; 3) change matrices; and 4) spatial trend maps. The change analyses revealed the changed or unchanged areas in terms of quantum, the LULC class trajectories and the trend that have occurred. The annual change rate was calculated in the equation (Li et al., 2017):

$$A_r (\%) = \frac{I_b - I_a}{I_b} \times \frac{1}{T} \times 100 \quad (6)$$

where;

A_r (%) is the annual change rate in percentage,

I_b is the area at the beginning and

I_a is the end of land use class,

T is the time period.

A spatial trend analysis which reveal the direction of the LULC change was generated from the 1986-2013 and 2013-2023 LULC maps. This study used a

Table 4. Error matrix and kappa (K^{\wedge}) statistics of image classification.

2023 ACCURACY REPORT					
Class Name	Reference Totals	Classified Totals	Number Correct	Producers Accuracy	Users Accuracy
Built-Up	75	78	72	96.00%	92.31%
Close Forest	14	15	12	85.71%	80.00%
Open Forest	64	64	56	87.50%	87.50%
Farmland	40	36	31	77.50%	86.11%
Water	10	10	10	100.00%	100.00%
Totals	203	203	181		
Overall Classification Accuracy = 89.16%					
2013 ACCURACY REPORT					
Class Name	Reference Totals	Classified Totals	Number Correct	Producers Accuracy	Users Accuracy
Built-Up	48	48	42	87.50%	87.50%
Close Forest	13	16	11	84.62%	68.75%
Open Forest	81	81	73	90.12%	90.12%
Farmland	48	45	38	79.17%	84.44%
Water	10	10	10	100.00%	100.00%
Totals	200	200	174		
Overall Classification Accuracy = 87.00%					
KAPPA (K^{\wedge}) STATISTICS					
Conditional Kappa for each Category					
Class Name	2013 Kappa	2023 Kappa			
Built-Up	0.8355	0.878			
Close Forest	0.6658	0.7852			
Open Forest	0.834	0.8174			
Farmland	0.7953	0.827			
Water	1	1			
Overall Kappa Statistics	0.8186	0.8487			

polynomial to analysis the spatial trend for the two (2) different periods. The spatial trend analyses were based on effect of other LU classes on built-up LU class.

Urban Sprawl Analysis

Extracting the built-up areas spatial extent has become one of the essential fac-

tors relating to build environment to catalog its development through time. It revealed how they physically expand (Katsoulakos et al., 2016). In determining urban sprawl, the 1986, 2013 and 2023 LULC data were evaluated. The extracted built-up areas from the 3 LULC maps coupled with the road network were superimposed on each other. The resultant map revealed levels of the direction of spatial expansion of the built-up areas within the study area (Figure 3).

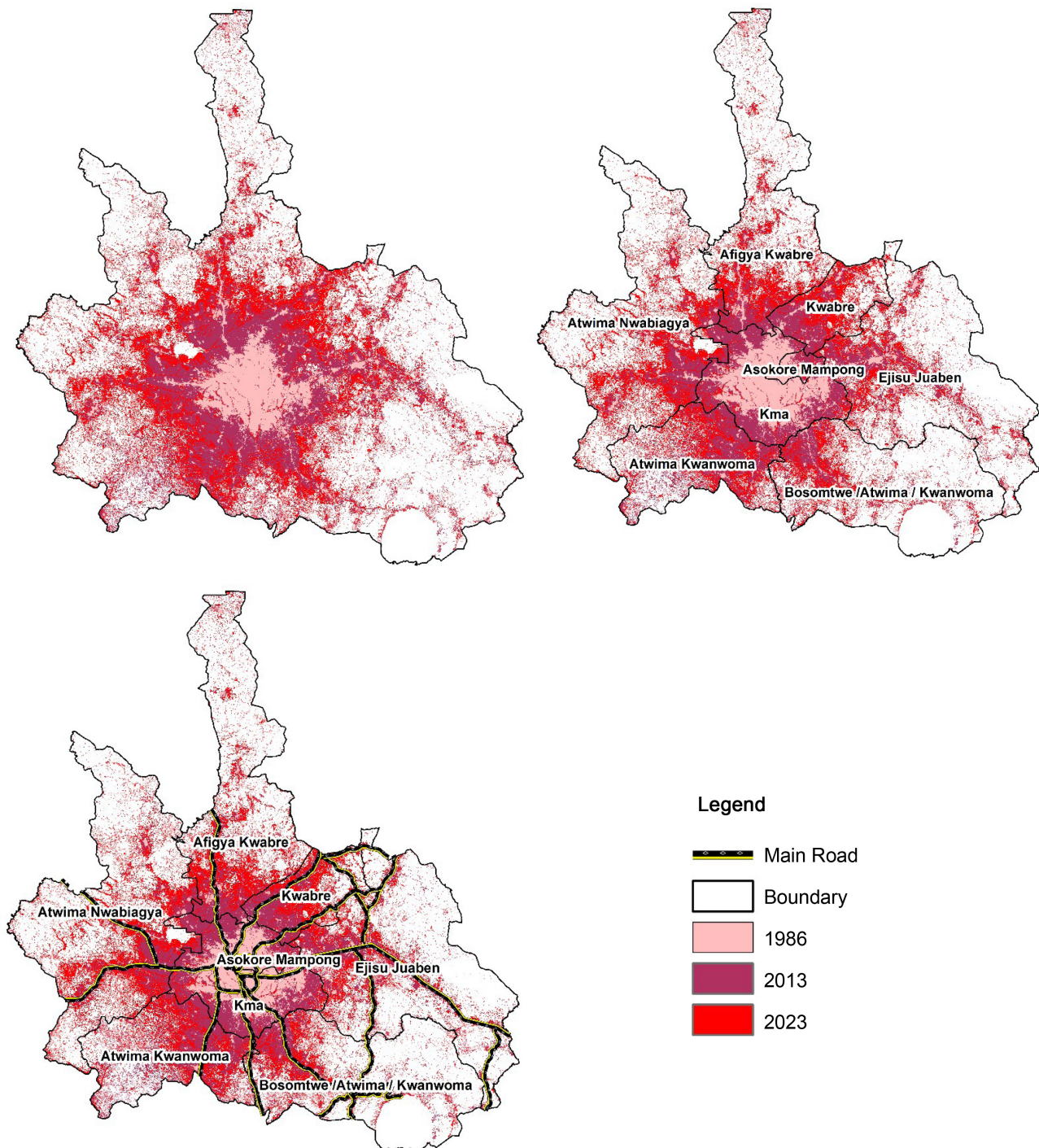


Figure 3. Urban extent maps for 1986, 2013, 2023.

To measure the urban sprawl type of study area, the area of all the LULC classes from the LULC maps for the three periods: 1986, 2013 and 2023 were computed and analyzed. The study adopt Shannon's entropy formula to measure the sprawl within the period under review. The Shannon entropy (En) is computed by:

$$En = -\sum_{i=1}^n P_i \log(P_i) / \log(n) \quad (7)$$

where P_i is the area of each LULC classes in decimal and n is the total number of LULC classes.

3. Results

3.1. LULC Maps and Quantification

This study adopted supervised image classification based on MLC algorithm in classifying the study area into five (5) LULC (**Table 5**). **Table 5** indicates the amount LULC of each category measured in hectares (ha) and their various percentages. **Figure 4** depicts the three classified maps of the study area generated from 1986, 2013 and 2023 satellite images and these figures show substantial modification from one type to another type. The dominant LULC class within the study area in 1986 was the open forest (64.34%) and remains as the dominant class in 2013 as well. In 2023, the built-up area experienced much expansion (41%) at the expense of other LU classes. Although the study area is drained by several streams and rivers, it could not be revealed because of the spatial resolution of the Landsat images. Only the dams and the lake within the study area were conspicuous and therefore mapped. Water class area coverage was the lowest (2%) among the classes.

Table 5 reveals that in 1986 and 2013, Open Forest class was the major LULC class within the representing 64.34% and 34.18% respectively but was overtaken by built-up (41.0%) LULC class in 2023. In 2023, it is noticed that the depreciation of Open Forest LULC class slowed down to 32.75% area coverage. The Close Forest LU Class which is designated as a protected area in the study area, increased slightly from 9.12% to 10.93% from the 1986 to 2013 but there was a sharp loss to 4.35% in 2023. The sharp declining of the Open Forest from the

Table 5. Quantification of land use land cover classes.

	1986 LU		2013 LU		2023 LU	
	ha	%	ha	%	ha	%
Built-Up	228,410	8.04	636,357	22.39	1,165,393	41.00
Close Forest	259,350	9.12	310,583	10.93	123,511	4.35
Open Forest	1,828,783	64.34	971,460	34.18	930,814	32.75
Farmland	467,518	16.45	865,905	30.46	565,360	19.89
Water	58,433	2.06	58,189	2.05	57,416	2.02
Total	2,842,494	100	2,842,494	100	2,842,494	100

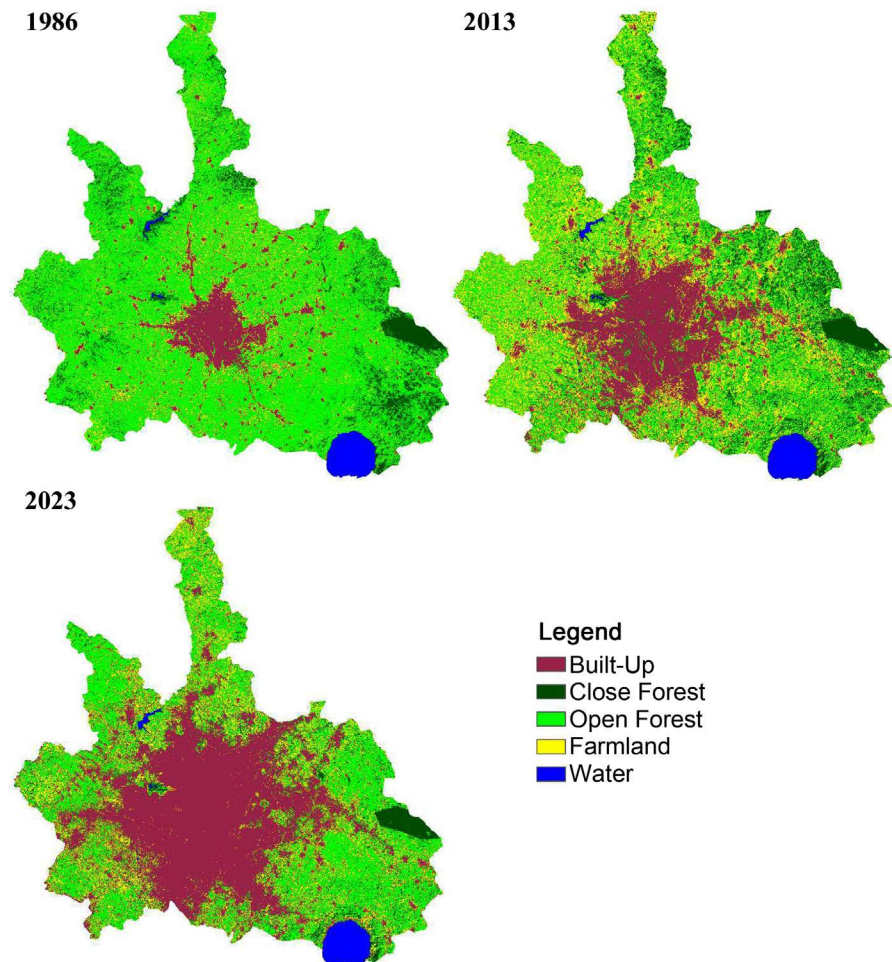


Figure 4. LULC maps for the Epoch years.

1986 to 2013 has been attributed the high level of deforestation because of high population, illegal cutting down of trees, mining and unsustainable farming methods.

3.2. Accuracy Assessment

Accuracy assessment produced from the 2013 and 2023 LULC maps were performed from 200 validation data and assessment reports generated (Table 4). Total classification accuracy of 89.16% and 87% were attained for 2013 and 2023 respectively. Its corresponding overall Kappa value of 0.8186 and 0.8487 were attained respectively.

3.3. Change Analysis

The study area revealed significant changes within the two-time periods (1986-2013 & 2013-2023). Figure 5 shows the net gains or loss within the two-time period. The change maps are shown in Figure 6. The two (2) change matrices (1986-2013) and (2013-2023) are shown in Table 6 & Table 7. From the change matrices, the area highlighted yellow (diagonals) refers to areas that

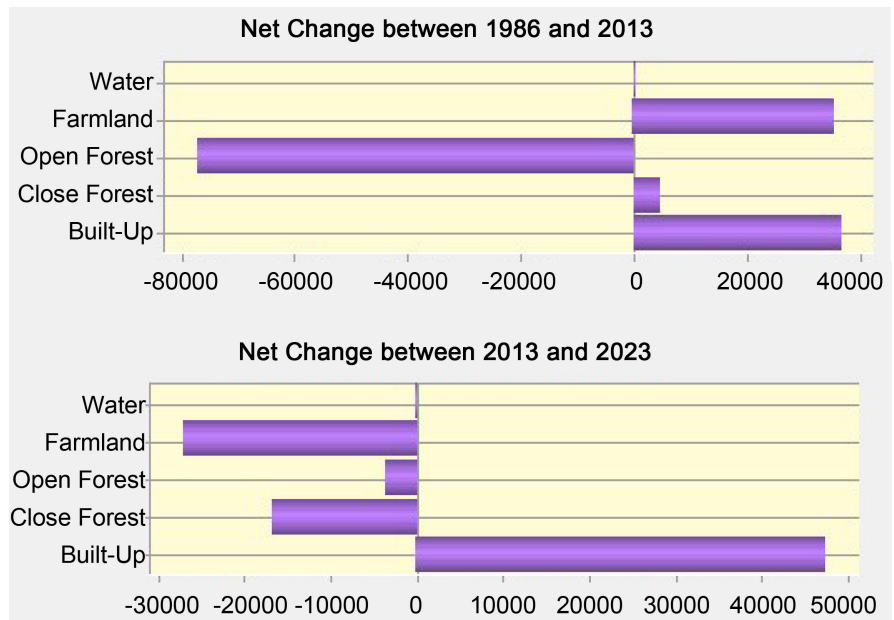


Figure 5. LULCC maps for 1986-2013 & 2013-2023.

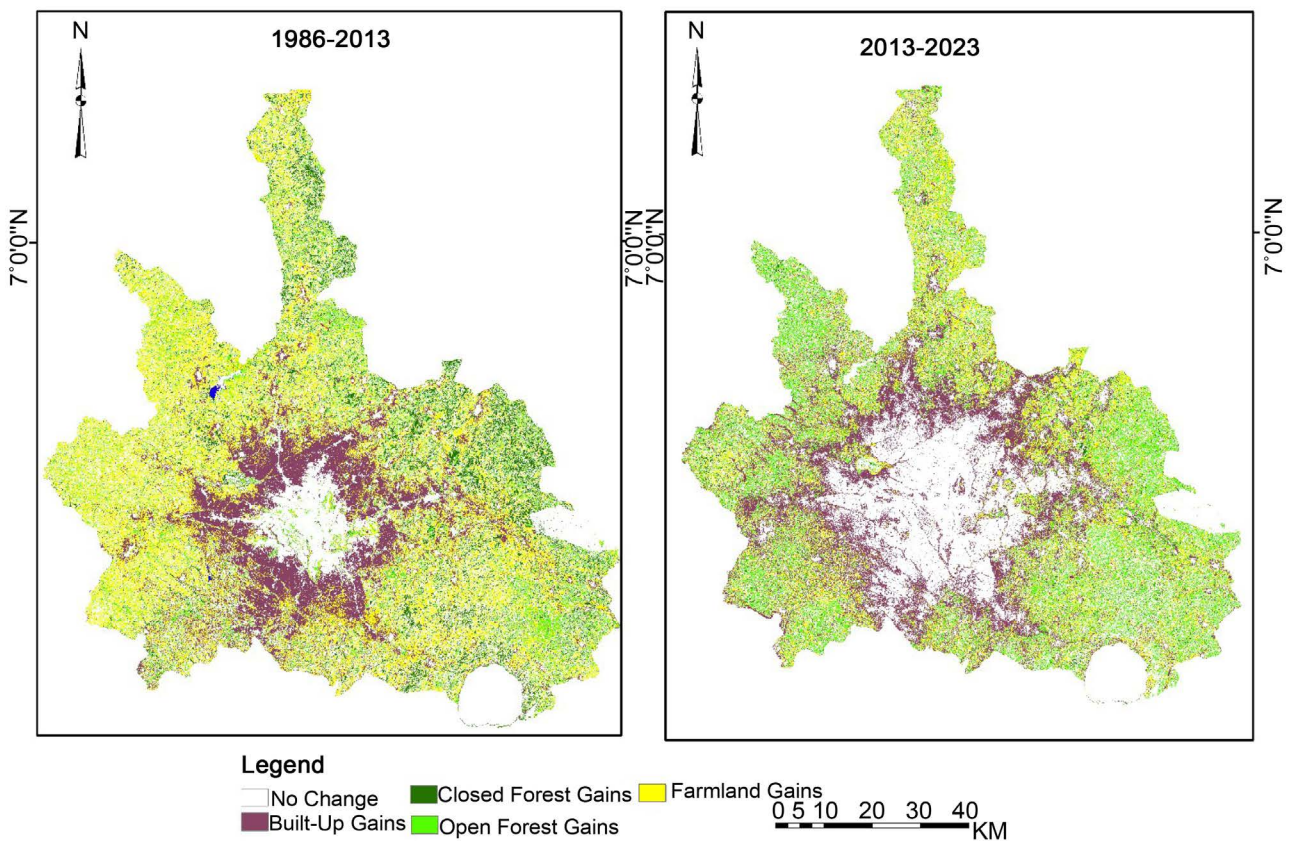


Figure 6. LULCC maps for 1986-2013 & 2013-2023.

remain unchanged and the off diagonals refers to areas that have experienced changes. Figure 5 indicate that in the period 1986-2013, only Open Forest experienced net loss of 30% as compared to other LU classes with built-up and

Table 6. Change detection 1986-2013 and 2013-2023.

		1986 LU					
		Built-Up	Close Forest	Open Forest	Farmland	Water	Total
2013 LU	Built-Up	187,528	3963	315,910	128,741	215	636,357
	Close Forest	1304	98,848	179,471	29,818	1142	310,583
	Open Forest	17,449	103,810	700,580	149,192	429	971,460
	Farmland	22,123	51,878	631,963	159,719	222	865,905
	Water	6	851	859	48	56,425	58,189
	Total	228,410	259,350	1,828,783	467,518	58,433	2,842,494

Table 7. Change detection 2013-2023.

		2013 LU					
		Built-Up	Close Forest	Open Forest	Farmland	Water	Total
2023 LU	Built-Up	579,720	29,183	233,128	323,182	180	1,165,393
	Close Forest	1172	83,902	28,926	8902	609	123,511
	Open Forest	27,914	134,999	449,533	318,308	60	930,814
	Farmland	27,539	62,449	259,860	215,492	20	565,360
	Water	12	50	13	21	57,320	57,416
	Total	636,357	310,583	971,460	865,905	58,189	2,842,494

farmland classes experiencing significant gains of 14%. Moreover, in the 2013-2023 period, it can be deduced that built-up areas continued to expand more (18.6%) at the expense of the remaining LU classes. This can be attributed to the fact that urbanization had rapidly taken place and massive development taken place affecting other LU classes within the study area. The other LU classes reduced substantially with farmland class reducing by 10.6% followed by closed forest 6.6% and the least by open forest 1.4% in 2023. It can be inferred from **Figure 5** that water class remains relatively stable as its experienced marginal changes within the study area.

According to **Table 5** and **Figure 5**, the built-up experienced much enlargement at the cost of other classes, mostly from Open Forest and Farmland LULC classes. Farmland is seen to have increased from 16.45% in 1986 to 30.46% in 2013 at the expense of Open Forest but strangely there was a sharp reduction to 19.89% in 2023. This can be related to the fact there have been a rapid population growth which resulted in the massive development taken place within the study area, converting nearby farmlands to built-up areas. Farmlands are therefore created from the two (2) forested areas by the populace. **Table 5** revealed that Close Forest coverage which is mainly protected areas and patches of tree

plantations within the study area is seen to have increased slightly from 9.12% in 1986 to 10.93% in 2013. However, it is seen to have declined sharply to 4.35% in 2023 indicating high deforestation rate within the study area. The Water LU class is seemed to be constantly stable in the study area as it seen to experience insignificant changes at 2% throughout the 3 time periods-1986, 2013 and 2023.

Table 6 and **Table 7** reveal the LULCC that have taken place within the two time periods 1986-2013 and 2013-2023 within the study area. These tables show how the conversions of the various LU classes happened. **Table 6** revealed that 60.3% of the total study area experienced changes within the period 1986-2013. Apart from Open Forest and Water LU classes, all other LU classes experienced gains within the period at a 2% annual growth rate of LULCC.

3.3.1. Spatial Trend Analysis

LULCC is attributed and sparked by urban spread. The transition from other LULC to the built-up category is seen. The expansion of built-up category on the other LULC class sparks the changes. **Figure 7** and **Figure 8** depict the spatial extent with other LU classes to built-up class. The spatial trend maps for 1986-2013 and 2013-2023 appear similar except the spatial trend of close forest

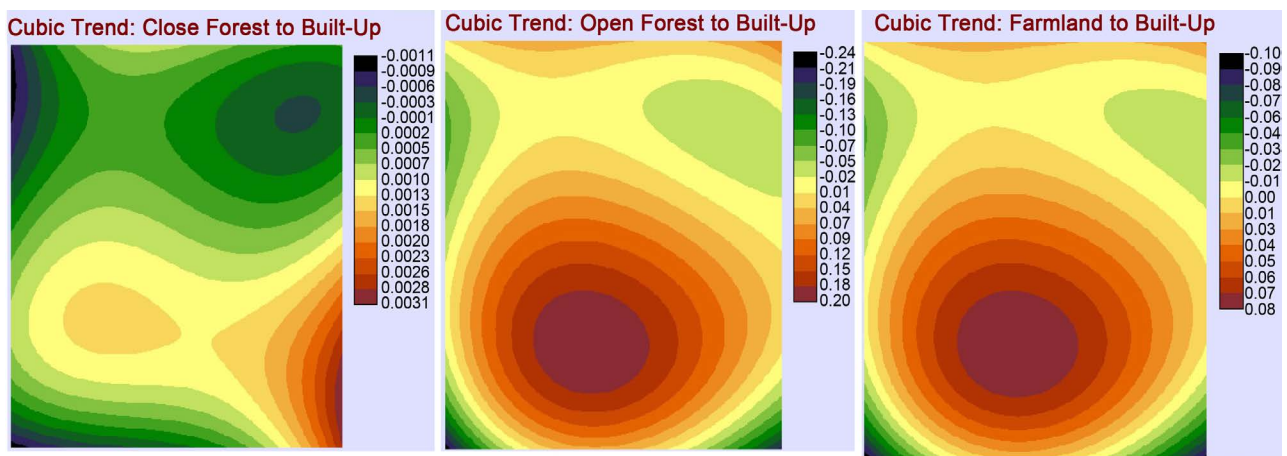


Figure 7. Urban spatial extent maps for 1986-2013.

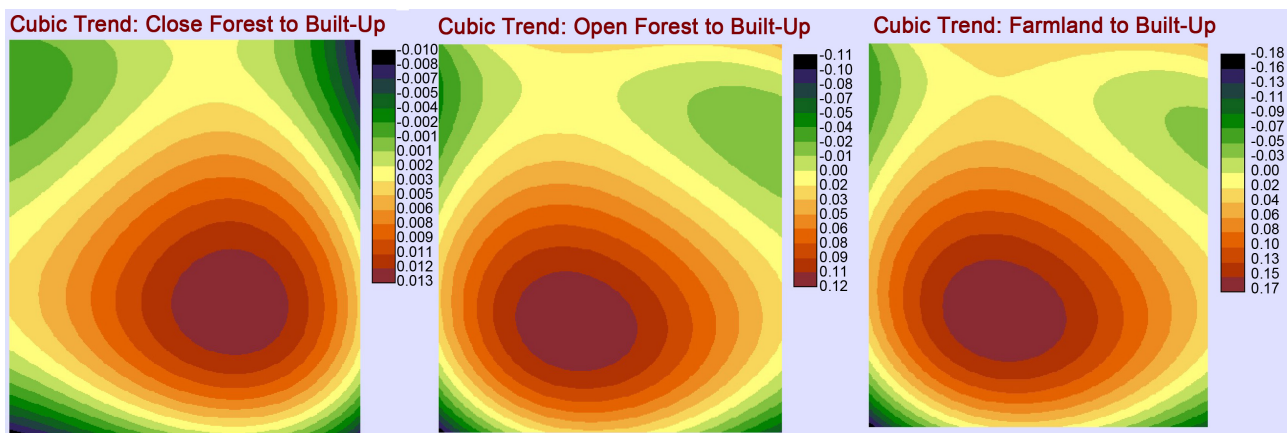


Figure 8. Urban spatial extent maps for 2013-2023.

to built-up which looks different. It can be deduced that the LULC classes at the central part in study area looks likely to transition to urban category than the fringe areas. The spatial trend of the change from all other LULC to the built-up class in the examined periods indicates correspondence with the trend of urban growth. It is expected that the trend of LULCC will move radially towards the corners.

Figure 3 shows the urban extent with the road networks of study area of the three years 1986, 2013 and 2023. It is revealed that urbanization was centrally expanding and along the road systems. Consequently, other LULC classes close to built-up areas were vulnerable to be transitioned to built-up areas than those at the fringes.

3.3.2. Urban Trends

The calculated entropy of the urban areas for 1986, 2013 and 2023 were 0.672, 0.861, and 0.788 respectively (**Table 8**). These values (entropy) imply that the greater Kumasi has undergone extensive urban sprawl as the entropy values approaches 1.

4. Discussion

4.1. LULC Maps and Accuracy Assessment

Supervised classification premised on MLC algorithm was utilized in classifying the Landsat images in the study. The MLC algorithm used has the ability to efficiently map LULC with high accuracies pertinent for monitoring LULCC (Shalaby & Tateishi, 2007; Huang et al., 2007). This algorithm supposes that the likelihoods are even for all groups and that the key bands have regular distribution with the merit of offering an index of confidence connected to the optimal of every pixel to the assumed group (Al-Ahmadi & Hames, 2009).

Foody (2002) and Behera et al. (2012) state the importance of accuracy assessment in post-classification change detection studies. Error Matrices and the kappa statistics (**Table 4**), the classification were therefore deemed to be accurate and satisfactory as the values attained falls within the threshold values 80% - 100% (Congalton, 1991; Firdaus et al., 2014).

The LULC maps confirm the reports that Ghana has a very high deforestation rate (Forestry Commission, 2015) The slowing down from 2013 to 2023 has been attributed to the governmental interventions, policies and strategies which been implemented to curtail such forest loss to achieve UN SDG (Forestry Commission of Ghana, 2016).

Table 8. Shannon's entropy values.

ID	Shannon's Entropy values (En)		
	1986	2013	2023
1	0.672	0.861	0.788

4.2. Change Analysis

The change analysis collaborates with earlier studies by [Forestry Commission. \(2015\)](#) and [Adu-Poku et al. \(2012\)](#). The sharply increment explained the fact that Ashanti region for that matter Kumasi (Capital) and its environs have experienced many developments within the last two decades ([Cobbinah, 2017](#)). Except for built-up LU class, all other class experienced losses with the Farmland LULC class suffering the most. This explains the fact that farmlands are closed to built-up areas as people tend to create farms at proximity. However, as urbanization grows people tend to develop areas at close proximity than fringe areas and thereby converting farmland areas into built ups ([Puplampu & Boafo, 2021](#); [Antwi et al., 2014](#)).

The study area has experienced forest loss within the 37-year period under review. Both of the forested areas is realized to have declined by about 50% of its land coverage within the time period 1986-2023. The main driving causes of this decline have been attributed to rapid urbanization and uncontrolled agricultural expansion ([Acheampong et al. 2019](#); [Koranteng et al., 2023](#); [Agyeman, 2012](#)).

4.3. Urbanization

The world is becoming increasingly urbanized. [United Nations Department of Economic and Social Affairs, Population Division \(2022\)](#) estimates that more than 50% of world's population resides in urban areas. In most of the developing world, most people in the rural areas keep migrating to the urban/cities in search for greener pasture to better their socio-economic life ([Sekher & Govil, 2022](#)). Kumasi, the capital of Ashanti has seen a rapid increase in population from 562,000 (1986) through to 2,354,000 (2013) to 3,768,000 (2023) at an average of 3.8% growth rate ([Sekher & Govil, 2022](#)). The figures represent the urban accumulation of Kumasi, which characteristically comprises Kumasi's population and adjoining districts. This study has confirmed that the built-up areas has increased more than 500% within the study area. This shows that more people from the rural areas have trooped in Kumasi and surrounding enclaves to experience city life and for improvement in economic condition. The comparatively massive social amenities in cities induce the movement of people from rural area to peri-urban areas. Most of these settlers reside in the periphery of the city (Kumasi) because of high accommodation costs and overcrowding ([Cobbinah & Amoako, 2012](#)). Unplanned urbanization because of rising economic activities impacts large tracts of natural environment negatively ([Owusu Ansah & Chigbu, 2020](#)).

Shannon's entropy determines how concentrated or dispersed the sprawl is occurring in the study area ([Yeh & Li, 2001](#); [Sudhira et al., 2004](#)). The entropy value ranges from 0 to 1, with value 0 indicating sprawling concentrated on one side and value approaching 1 when the sprawling is haphazardly dispersed within the area. The values obtained indicated urban sprawl in study area.

The results from this study portray the urban expansion in study area as more

sporadic and ribbon and reinforce an earlier paper by Cobbinah & Amoako (2012). Shannon's entropy values (Yeh & Li, 2001) showed less sprawl in 1986, increased in 2013 and declined slightly in 2023. Conclusively posit that the urban expansion is more dispersed within the study area. Fast and arbitrary built-up expansion account for the urban sprawl.

Mishra et al. (2018) reckoned that trend analysis as granting a visual opening to recognize likely directions of urban expansion. The results revealed the possible spatial trend of urbanization from the study area within the 37 years of review. The loss in agricultural land is one of the direct consequences of rapid urbanization and population growth (Xie et al., 2005). It is true in this study as the trend in urban growth has resulted into anthropogenic causes of farmland loss and the decline in forest cover in the study area.

5. Conclusion

The world of today is faced with several environmental challenges caused by either unavoidable natural or human-induced processes. However, anthropogenic activities have led to rapid environmental changes, which have resulted in several negative consequences such as unbridled urbanization, deforestation, climate change and food shortages. Consequently, an important component of environmental planning and management is to be able to monitor these rates and patterns of LULCC which are also related to environmental change.

Advanced RS and GIS procedures have provided excellent prospects and confirm substantial accomplishment in observing and overseeing LULCC.

The study has confirmed urbanization as the major factor of LULCC in the study area. Anthropogenetic-associated actions triggered the alarming escalation in built-up areas and the drastic decline of the farmlands and forested areas. It has become obvious that study area exhibits a more prevalence urban sprawl from the Shannon Entropy values computed. It is consequently, proposed that policy interventions require concerted efforts and should be executed collaboratively from all key stakeholders including the regional administration, traditional authorities, and central government to give extra impetus to the efforts in mitigating effect of these human induced changes to the LULC changes in Greater Kumasi area to prevent further destruction and to protect the remaining biodiversity and the ecological services. It is of great importance to direct all efforts in regulating and managing urban sprawl.

Acknowledgements

The authors thank the USGS for the provision of the free satellite images used in this work, Forestry Commission, Ghana, Survey & Mapping Division, Ghana. This study was supported by IDEA WILD of the USA with logistics such as laptop, GPS and Hard drives.

Conflicts of Interest

The authors declare no conflicts of interest regarding the publication of this paper.

References

- Acheampong, E. O., Macgregor, C. J., Sloan, S., & Sayer, J. (2019). Deforestation Is Driven by Agricultural Expansion in Ghana's Forest Reserves. *Scientific African*, *5*, e00146. <https://doi.org/10.1016/j.sciaf.2019.e00146>
- Adu-Poku, I., Drummond, J., & Li, Z. (2012). Land-Cover Change Monitoring in Obuasi, Ghana: An Integration of Earth Observation, Geoinformation Systems and Stochastic Modelling. *Journal of Earth Science and Engineering*, *2*, 1-14.
- Agyeman, K. O. (2012). Issues of Tropical Forest Transformation in Ashanti Region: Testing Traditional Perception and Assumption. *Journal of Science and Technology*, *32*, 79-95. <https://doi.org/10.4314/just.v32i1.9>
- Al-Ahmadi, F. S., & Al-Hames, A. S. (2009). Comparison of Four Classification Methods to Extract Land Use and Land Cover from Raw Satellite Images for Some Remote Arid Areas, Kingdom of Saudi Arabia. *Journal of King Abdulaziz University-Earth Sciences*, *20*, 167-191. <https://doi.org/10.4197/Ear.20-1.9>
- Anderson, J. R., Hardy, E. E., Roach, J. T., & Witmer, R. E. (1976). *A Land Use and Land Cover Classification System for Use with Remote Sensor Data* (Vol. 964). US Government Printing Office. <https://doi.org/10.3133/pp964>
- Antwi, E. K., Boakye-Danquah, J., Asabere, S. B., Yiran, G. A., Loh, S. K., Awere, K. G. et al. (2014). Land Use and Landscape Structural Changes in the Ecoregions of Ghana. *Journal of Disaster Research*, *9*, 452-467. <https://doi.org/10.20965/jdr.2014.p0452>
- Asabere, S. B., Acheampong, R. A., Ashiagbor, G., Beckers, S. C., Keck, M., Erasmi, S., Schanze, J., & Sauer, D. (2020). Urbanization, Land Use Transformation and Spatio-Environmental Impacts: Analyses of Trends and Implications in Major Metropolitan Regions of Ghana. *Land Use Policy*, *96*, Article ID: 104707. <https://doi.org/10.1016/j.landusepol.2020.104707>
- Asori, M., & Adu, P. (2023). Modeling the Impact of the Future State of Land Use Land Cover Change Patterns on Land Surface Temperatures Beyond the Frontiers of Greater Kumasi: A Coupled Cellular Automaton (CA) and Markov Chains Approaches. *Remote Sensing Applications: Society and Environment*, *29*, Article ID: 100908. <https://doi.org/10.1016/j.rsase.2022.100908>
- Atay Kaya, İ., & Kut Görgün, E. (2020). Land Use and Land Cover Change Monitoring in Bandırma (Turkey) Using Remote Sensing and Geographic Information Systems. *Environmental Monitoring and Assessment*, *192*, Article No. 430. <https://doi.org/10.1007/s10661-020-08411-1>
- Behera, M. D., Borate, S. N., Panda, S. N., Behera, P. R., & Roy, P. S. (2012). Modelling and Analyzing the Watershed Dynamics Using Cellular Automata (Ca)-Markov Model—A Geo-Information Based Approach. *Journal of Earth System Science*, *121*, 1011-1024. <https://doi.org/10.1007/s12040-012-0207-5>
- Benson, M. H. (2019). New Materialism. *Natural Resources Journal*, *59*, 251-280.
- Bufebo, B., & Elias, E. (2021). Land Use/Land Cover Change and Its Driving Forces in Shenkolla Watershed, South Central Ethiopia. *The Scientific World Journal*, *2021*, Article ID: 9470918. <https://doi.org/10.1155/2021/9470918>
- Cobbinah, P. B., & Amoako, C. (2012). Urban Sprawl and the Loss of Peri-Urban Land in Kumasi, Ghana. *International Journal of Social and Human Sciences*, *6*, e397.
- Cobbinah, P. B., & Niminga-Beka, R. (2017). Urbanisation in Ghana: Residential Land Use under Siege in Kumasi Central. *Cities*, *60*, 388-401. <https://doi.org/10.1016/j.cities.2016.10.011>
- Congalton, R. G. (1991). A Review of Assessing the Accuracy of Classifications of Re-

- motely Sensed Data. *Remote Sensing of Environment*, 37, 35-46.
[https://doi.org/10.1016/0034-4257\(91\)90048-B](https://doi.org/10.1016/0034-4257(91)90048-B)
- Firdaus, R., Nakagoshi, N., & Idris, A. (2014). Sustainability Assessment of Humid Tropical Watershed: A Case of Batang Merao Watershed, Indonesia. *Procedia Environmental Sciences*, 20, 722-731. <https://doi.org/10.1016/j.proenv.2014.03.086>
- Foody, G. M. (2002). Status of Land Cover Classification Accuracy Assessment. *Remote Sensing of Environment*, 80, 185-201. [https://doi.org/10.1016/S0034-4257\(01\)00295-4](https://doi.org/10.1016/S0034-4257(01)00295-4)
- Forestry Commission (2015). *National REDD+ Strategy*. Report Prepared by Prize Water House Coopers for the Forestry Commission of Ghana, Forestry Commission.
- Forestry Commission of Ghana (2016). *Forestry Development Master Plan 2016-2036*. <https://www.fao.org/faolex/results/details/en/c/LEX-FAOC174385/>
- Frimpong, B. F., Koranteng, A., Atta-Darkwa, T., Junior, O. F., & Zawila-Niedźwiecki, T. (2023). Land Cover Changes Utilising Landsat Satellite Imageries for the Kumasi Metropolis and Its Adjoining Municipalities in Ghana (1986-2022). *Sensors*, 23, Article No. 2644. <https://doi.org/10.3390/s23052644>
- Ghana Statistical Service (GSS) (2022). *Ghana 2021 Population and Housing Census General Report Volume 3E: Economic Activity*. Ghana Statistical Service.
- Grigorescu, I., Kucsicsa, G., Popovici, E. A., Mitrică, B., Mocanu, I., & Dumitrașcu, M. (2021). Modelling Land Use/Cover Change to Assess Future Urban Sprawl in Romania. *Geocarto International*, 36, 721-739. <https://doi.org/10.1080/10106049.2019.1624981>
- Hersperger, A. M., Oliveira, E., Pagliarin, S., Palka, G., Verburg, P., Bolliger, J., & Grădinaru, S. (2018). Urban Land-Use Change: The Role of Strategic Spatial Planning. *Global Environmental Change*, 51, 32-42. <https://doi.org/10.1016/j.gloenvcha.2018.05.001>
- Huang, H., Legarsky, J., & Othman, M. (2007). Land-Cover Classification Using Radarsat and Landsat Imagery for St. Louis, Missouri. *Photogrammetric Engineering & Remote Sensing*, 73, 37-43. <https://doi.org/10.14358/PERS.73.1.37>
- Ioja, C., & Qureshi, S. (2020). Urban Wildland—Forests, Waters and Wetlands. In J. Breuste, M. Artmann, C. Ioja, & S. Qureshi (Eds.), *Making Green Cities. Cities and Nature* (pp. 177-287). Springer. https://doi.org/10.1007/978-3-030-37716-8_5
- Kamusoko, C. (2019). Pre-Processing. In C. Kamusoko (Ed.), *Remote Sensing Image Classification in R* (pp. 25-66). Springer. https://doi.org/10.1007/978-981-13-8012-9_2
- Katsoulakos, N. M., Misthos, L. M., Doulos, I. G., & Kotsios, V. S. (2016). Environment and Development. In S. G. Pouloupoulos, & V. J. Inglezakis (Eds.), *Environment and Development* (pp. 499-569). Elsevier. <https://doi.org/10.1016/B978-0-444-62733-9.00008-3>
- Khelifi, L., & Mignotte, M. (2020). Deep Learning for Change Detection in Remote Sensing Images: Comprehensive Review and Meta-Analysis. *IEEE Access*, 8, 126385-126400. <https://doi.org/10.1109/ACCESS.2020.3008036>
- Koranteng, A., Adu-Poku, I., Donkor, E., & Zawila-Niedźwiecki, T. (2020). Geospatial Assessment of Land Use and Land Cover Dynamics in the Mid-Zone of Ghana. *Folia Forestalia Polonica, Series A: Forestry*, 62, 288-305. <https://doi.org/10.2478/ffp-2020-0028>
- Koranteng, A., Frimpong, B. F., Adu-Poku, I., Asamoah, J. N., & Zawila-Niedźwiecki, T. (2023). Assessment of Past and Future Land Use/Land Cover Dynamics of the Old Kumasi Metropolitan Assembly and Atwima Nwabiagya Municipal Area, Ghana. *Journal of Geoscience and Environment Protection*, 11, 44-69. <https://doi.org/10.4236/gep.2023.113004>
- Koranteng, A., Poku, I. A., Donkor, E., & Niedźwiecki, T. Z. (2021). Multi-Temporal

- Study of Land Use Land Cover Changes. *International Journal of Environmental Sciences & Natural Resources*, 29, Article ID: 556254. <https://doi.org/10.19080/IJESNR.2021.29.556254>
- Li, Y., Liu, G., & Huang, C. (2017). Dynamic Changes Analysis and Hotspots Detection of Land Use in the Central Core Functional Area of Jing-Jin-Ji from 2000 to 2015 Based on Remote Sensing Data. *Mathematical Problems in Engineering*, 2017, Article ID: 2183585. <https://doi.org/10.1155/2017/2183585>
- Makwinja, R., Kaunda, E., Mengistou, S., & Alamirew, T. (2021). Impact of Land Use/Land Cover Dynamics on Ecosystem Service Value—A Case from Lake Malombe, Southern Malawi. *Environmental Monitoring and Assessment*, 193, Article No. 492. <https://doi.org/10.1007/s10661-021-09241-5>
- Mishra, V. N., Rai, P. K., Prasad, R., Punia, M., & Nistor, M. M. (2018). Prediction of Spatio-Temporal Land Use/Land Cover Dynamics in Rapidly Developing Varanasi District of Uttar Pradesh, India, Using Geospatial Approach: A Comparison of Hybrid Models. *Applied Geomatics*, 10, 257-276. <https://doi.org/10.1007/s12518-018-0223-5>
- Morshed, S. R., Fattah, M. A., Haque, M. N., & Morshed, S. Y. (2022). Future Ecosystem Service Value Modeling With Land Cover Dynamics by Using Machine Learning Based Artificial Neural Network Model for Jashore City, Bangladesh. *Physics and Chemistry of the Earth, Parts A/B/C*, 126, Article ID: 103021. <https://doi.org/10.1016/j.pce.2021.103021>
- Muhammed, E. M., & Emigilati, M. A. (2019). Socio Economic Impact of Urban Sprawl on Agricultural Land in Lapai Local Government Area, Niger State, Nigeria. *African Scholar Journal of Agriculture and Agricultural Technology*, 15, 109-126
- Naboureh, A., Bian, J., Lei, G., & Li, A. (2021). A Review of Land Use/Land Cover Change Mapping in the China-Central Asia-West Asia Economic Corridor Countries. *Big Earth Data*, 5, 237-257. <https://doi.org/10.1080/20964471.2020.1842305>
- Olorunfemi, I. E., Fasinmirin, J. T., Olufayo, A. A., & Komolafe, A. A. (2020). GIS and Remote Sensing-Based Analysis of the Impacts of Land Use/Land Cover Change (LULCC) on the Environmental Sustainability of Ekiti State, Southwestern Nigeria. *Environment, Development and Sustainability*, 22, 661-692. <https://doi.org/10.1007/s10668-018-0214-z>
- Owusu Ansah, B., & Chigbu, U. E. (2020). The Nexus between Peri-Urban Transformation and Customary Land Rights Disputes: Effects on Peri-Urban Development in Trede, Ghana. *Land*, 9, Article No. 187. <https://doi.org/10.3390/land9060187>
- Pal, S., Singha, A., Mondal, S., & Debanshi, S. (2023). Ecological Consequences of Urban Blue Space Transformation. *Environmental Science and Pollution Research*, 30, 34115-34134. <https://doi.org/10.1007/s11356-022-24575-4>
- Peng, X., Zhong, R., Li, Z., & Li, Q. (2020). Optical Remote Sensing Image Change Detection Based on Attention Mechanism and Image Difference. *IEEE Transactions on Geoscience and Remote Sensing*, 59, 7296-7307. <https://doi.org/10.1109/TGRS.2020.3033009>
- Phiri, D., Morgenroth, J., Xu, C., & Hermosilla, T. (2018). Effects of Pre-Processing Methods on Landsat OLI-8 Land Cover Classification Using OBIA and Random Forests Classifier. *International Journal of Applied Earth Observation and Geoinformation*, 73, 170-178. <https://doi.org/10.1016/j.jag.2018.06.014>
- Puplampu, D. A., & Boafo, Y. A. (2021). Exploring the Impacts of Urban Expansion on Green Spaces Availability and Delivery of Ecosystem Services in the Accra Metropolis. *Environmental Challenges*, 5, Article ID: 100283. <https://doi.org/10.1016/j.envc.2021.100283>

- Richards, J. A. (1999). *Remote Sensing Digital Image Analysis* (240 p.). Springer.
- Sekher, T. V., & Govil, D. (2022). *World Population Day-2022 Symposium & Launch of United Nations World Population Prospects-2022*. International Institute for Population Sciences.
- Shalaby, A., & Tateishi, R. (2007). Remote Sensing and GIS for Mapping and Monitoring Land Cover and Land Use Changes in the Northwestern Coastal Zone of Egypt. *Applied Geography*, 27, 28-41. <https://doi.org/10.1016/j.apgeog.2006.09.004>
- Shi, W., Zhang, M., Zhang, R., Chen, S., & Zhan, Z. (2020). Change Detection Based on Artificial Intelligence: State-of-the-Art and Challenges. *Remote Sensing*, 12, Article No. 1688. <https://doi.org/10.3390/rs12101688>
- Sibanda, S., & Tsuyuki, S. (2022). Identifying the Rates and Drivers of Spatiotemporal Patterns of Land Use and Land Cover Changes in the Hurungwe District, Zimbabwe: A GIS and Remote Sensing Approach. *Journal of Geographic Information System*, 14, 652-679. <https://doi.org/10.4236/jgis.2022.146037>
- Sudhira, H. S., Ramachandra, T. V., & Jagadish, K. S. (2004). Urban Sprawl: Metrics, Dynamics and Modelling Using GIS. *International Journal of Applied Earth Observation and Geoinformation*, 5, 29-39. <https://doi.org/10.1016/j.jag.2003.08.002>
- Sun, H., Forsythe, W., & Waters, N. (2007). Modeling Urban Land Use Change and Urban Sprawl: Calgary, Alberta, Canada. *Networks and Spatial Economics*, 7, 353-376. <https://doi.org/10.1007/s11067-007-9030-y>
- United Nations Department of Economic and Social Affairs, Population Division (2022). *World Population Prospects 2022: Summary of Results*. UN DESA/POP/2022/TR/NO. 3.
- Weslati, O., Bouaziz, S., & Sarbeji, M. M. (2023). Modelling and Assessing the Spatiotemporal Changes to Future Land Use Change Scenarios Using Remote Sensing and CA-Markov Model in the Mellegue Catchment. *Journal of the Indian Society of Remote Sensing*, 51, 9-29. <https://doi.org/10.1007/s12524-022-01618-4>
- Wiatkowska, B., Słodczyk, J., & Stokowska, A. (2021). Spatial-Temporal Land Use and Land Cover Changes in Urban Areas Using Remote Sensing Images and GIS Analysis: The Case Study of Opole, Poland. *Geosciences*, 11, Article No. 312. <https://doi.org/10.3390/geosciences11080312>
- Xie, Y., Mei, Y., Tian, G., & Xing, X. (2005). Socio-Economic Driving Forces of Arable Land Conversion: A Case Study of Wuxian City, China. *Global Environmental Change*, 15, 238-252. <https://doi.org/10.1016/j.gloenvcha.2005.03.002>
- Yeh, A., & Li, X. (2001). Measurement and Monitoring of Urban Sprawl in a Rapidly Growing Region Using Entropy. *Photogrammetric Engineering and Remote Sensing*, 67, 83-90.